Reliability assessment on ultimate and serviceability limit states and determination of critical factor of safety for underground rock caverns

Zhang, Wengang; Goh, Anthony Teck Chee

2012

Zhang, W., & Goh, A. T. C. (2012). Reliability assessment on ultimate and serviceability limit states and determination of critical factor of safety for underground rock caverns. Tunnelling and Underground Space Technology, 32, 221-230.

https://hdl.handle.net/10356/95168

https://doi.org/10.1016/j.tust.2012.07.002

Reliability assessment on ultimate and serviceability limit states and determination of critical factor of safety for underground rock caverns

Wengang Zhang, Anthony T. C. Goh*

School of Civil and Environmental Engineering, Nanyang Technological University, 639798 Singapore, Singapore

ABSTRACT

The observational design method which uses extensometers to measure the displacements during cavern construction and then adopt these data for back analysis does not always guarantee satisfactory performance because the displacements provide little information about the strength to stress ratio that ultimately determines the stability of the rock caverns. In this study, both the ultimate and serviceability limit states are investigated by means of the Finite Difference program FLAC^{3D}. The global factor of safety obtained using the shear strength reduction technique is used as the criterion for the ultimate limit state and the calculated percent strain around the opening is adopted as the serviceability limit state criterion. High deformability, low shear strength and the high in-situ stress state are the major factors that govern the underground rock cavern stability and serviceability. Through the identification of the key influencing parameters for calculating the factor of safety and the percent strain, numerical experimentations are performed in accordance with the methodology of 2^k factorial design, from which polynomial regression models are developed for each rock mass condition. The First-Order Reliability Method (FORM) was used to determine the probability of failure for the limit states. Through the use of the automated spreadsheet search algorithm to determine the design point, to meet the different target performance levels, the required minimum *FS* is obtained and termed as the critical value. This

*Corresponding author Tel.: +65 6790 5271. Fax: +65 6792 0676

E-mail address: ctcgoh@ntu.edu.sg

proposed approach enables a cost-effective analysis to be conducted for a rational design of underground rock caverns.

Keywords: reliability assessment; serviceability limit state; ultimate limit state; factor of safety; percent strain; target performance level.

1. Introduction

It is geotechnical practice and also a fact that the deterministic global factor of safety (*FS*) provides a hedge against uncertainties in calculation and is infrequently computed with accuracy. Through engineering experience, conventions have been defined concerning the suitable values of factor of safety for various situations. However, in the literature few contributions deal with a proper choice for underground rock caverns under different rock mass conditions.

The current design of geotechnical structures uses deterministic methods to obtain a global *FS* in relation to the various limit states. The stochastic nature of the design parameters is usually not considered.

In this paper, the failure is interpreted in the most general sense, i.e., the cavern performance is unsatisfactory as a result of instability (collapse) or excessive movements. Collapse refers to ultimate limit state failure, in which the stresses exceed the capacities of the rock or structural elements. Excessive movements, which will cause difficulties during excavation such as lining placement and reinforcement installation, refer to the failure of the serviceability limit state. Both these two distinct failures should be prevented in the design. Conventional deterministic evaluation of stability of geotechnical structures and underground openings involves the calculation of *FS*. This single FS value can neither quantify the margin of safety with absolute certainty nor meet the serviceability requirements. For the serviceability limit requirement, numerically this is assessed either by the calculated displacements or strains, the plastic zone volume or the yielding zone radius. Field instrumentation and monitoring are usually considered in the observational design method to check the tunnel / cavern performance by means of multiple-position borehole extensometers (MPBX). Usually the strain gauges are instrumented to check the performance of the rock bolts by measuring the bolt loads. A strain distribution of reasonable accuracy can be used for safety assessment for different construction stage (Sakurai et al., 2003). Moreover, if a threshold for the strain values is defined, one can modify the support system according to the in-situ observations as the project advances

(Sharifzadeh et al., 2011).

Probabilistic design approaches may take uncertainties and complexities into account. In this paper, a stochastic design approach is proposed ensuring that the ultimate and serviceability limit requirements are both met. In addition, it satisfies the expected performance level, which is quantified through a reliability index β. Typical values for β and probability of failure P_f for representative geotechnical components and systems and their expected performance levels have been proposed (U.S. Army Corps of Engineers., 1997), as shown in Table 1.

Table 1

It is suggested herein a threshold value of percent strain at the cavern periphery exists above which the serviceability limit state is not satisfied. This limit value is the critical strain. The observed or expected strain at the opening depends on the ground conditions, which are classified through the Rock Mass Rating (*RMR*) and, in addition, on size and shape of the opening and in-situ stresses.

This paper focuses on the development of a mathematical expression relating *FS* to the rock mass strength parameters and another expression relating percent strain to various rock mass properties. The objective of this study is also to explore the feasibility of defining satisfactory performances that meet both the ultimate and serviceability limit states.

2. Design methods for rock caverns

Empirical (Rock Mass Classification system, RMC) and numerical methods are commonly used tools for the design of underground structures. The *RMR* (Bieniawski, 1973, 1974) is one of the most widely used empirical systems. Different *RMR* values are assigned to characterize different rock mass conditions. However, *RMR* cannot adequately characterize the stress redistribution and deformation around an opening (Basarir, 2008). Thus a Finite Difference program is used to derive the global *FS* and the percent strain in this study. In the following the probabilistic approach to be used for a preliminary design is described.

2.1. Estimation of rock mass strength parameters

In the preliminary stage of an engineering design, the need for an approximate estimate of the rock mass parameters frequently arises (Bieniawski, 1978; Barton et. al. 1980; Hoek and Brown, 1997; Palmstrom and Broch, 2006; Basarir, 2006; Aksoy et al., 2010). For the finite difference analyses carried out in this study, the following equations (Equations 1-5) are adopted for determining the rock mass properties.

$$E_m(GPa) = 10^{\frac{RMR-10}{40}} \quad \text{(Serafim and Pereira, 1983)} \tag{1}$$

$$c(MPa) = 0.005(RMR - 1.0) \quad \text{(Bieniawski, 1989)} \tag{2}$$

$$\phi(^\circ) = 0.5RMR + 4.5 \quad \text{(Bieniawski, 1989)} \tag{3}$$

$$\sigma_{cm}(MPa) = 0.5e^{0.06RMR} \quad \text{(Trueman, 1988)} \tag{4}$$

$$\sigma_t(MPa) = \frac{\sigma_{cm}}{10} \tag{5}$$

where E_m is the deformation modulus of rock mass, c is the cohesive strength, ϕ is the friction angle, σ_{cm} is the Uniaxial Compressive Strength (*UCS*) and σ_t is the tensile strength. For fair to very good rock mass, the corresponding *RMR* values are in the range of 50-90. The *RMR* values and corresponding rock mass class and empirical estimates of rock strength mean values are reported in Table 2. In the analyses, densities of 2430 kg / m^3, 2610 kg / m^3 and 2630 kg / m^3 are assumed for average *RMR* values of 50, 70 and 90, respectively. A Poisson's ratio of 0.24 is assumed for all the ranges of *RMR*.

Table 2

2.2. The 2^4 factorial design and fixing design levels

As shown in Table 2, E_m, c and ϕ are treated as random variables for each *RMR* (rock class) considering that high deformability, low shear strength and the high in-situ stress state are the major factors that govern the underground rock cavern stability and serviceability. In view of the fact that the in-situ stress substantially influences the cavern stability and serviceability, K_0 is also taken into consideration. However, unlike

the other three parameters, K_0 is independent on *RMR*. In order to assess the influence of the random (input) variables on the output (either *FS* or percent strain), the factorial design approach commonly used in statistical analysis was adopted (Montgomery 2001). For a problem with k random variables, the 2^k factorial design provides the minimum number of analyses with which k factors can be studied to assess the relationship between the random input variables and the output. In the present study, rock mass parameters E_m, c and ϕ and in-situ stress ratio K_0 each at two levels (high and low levels) are considered as the four design factors (input variables). The high level and low level values are related to mean value μ and the standard deviation σ by means of the relationships $x_h = \mu + 1.645\sigma$ and $x_l = \mu - 1.645\sigma$ respectively. These values are based on the assumption that the input parameters follow the normal distribution. For each random variable, two design combinations are considered and denoted by the '+' and '–' notations to represent the high and low values of each stochastic input variable. Table 3 summarizes the four design factors considered. Standard notations are followed to provide clarity with regard to the various terms involved in the factorial design.

Table 3

2.3. Numerical experimentations

The FLAC^{3D} code (Itasca, 2005) was utilized for the numerical experiments. The Mohr-Coulomb constitutive model was selected for the rock. The cross-section of the cavern, the side view and the boundary conditions are shown in Fig.1. The cavern roof is semi-circular and the cavern dimensions are: height of the roof 15 m, wall height 15 m and cavern span 30 m. The plane-strain conditions are enforced by including a thin 1 m slice of material in the longitudinal direction and imposing boundary conditions on the two off-plane surfaces that allow movement vertically but are restrained against displacements normal to these planes. Outer boundaries are located far from the cavern wall. The overburden height D from the ground surface to the top of the side wall is 100 m. No surface loading above-ground surface is considered. The initial vertical in-situ stress σ_v is induced by self-weight of the rock. The horizontal stress σ_h is calculated using $K_0 \times \sigma_v$. A full-face excavation is considered.

Fig. 1.

The numerical results include the factor of safety and the percent strain. *FS* is solved through the Shear Strength Reduction (SSR) technique (also called *c*-ϕ-reduction method), in which the shear strengths are systematically reduced until failure occurs. This procedure was proposed by Zienkiewicz et al. (1975), and improved by Brinkgreve and Bakker (1991). It has been applied to caverns (Hammah et al., 2007), circular tunnels in homogeneous ground (Vermeer and Ruse, 2002) and tunnel face stability problems (Vermeer et al., 2002). The percent strain ε is the maximum value among the values of average strain ε_{Mm} of peripheral elements around the cavern. Strain ε_{Mm} is calculated as follows (Sakurai, 1997a):

$$\varepsilon_{Mm}(\%) = \frac{u_M - u_m}{l_{Mm}} \times 100 \tag{6}$$

and the percent strain is:

$$\varepsilon = \max(\varepsilon_{Mm}, \varepsilon_{Nn}, \varepsilon_{Pp}, \varepsilon_{Qq}, \varepsilon_{Ss} \cdots) \tag{7}$$

given u_M displacement of a peripheral node M, u_m displacement of corresponding inner node m and l_{Mm} length between nodes M and m (Fig. 1). It should be noted that the selected length of l_{Mm} is typical of many extensometers and the locations of inner nodes such as m are chosen at the grid of the third layer elements around the opening. Numerical trials carried out on different locations of inner nodes and different mesh densities indicate that the choice of the reference length and the density of mesh at the opening have the minimal influence on the magnitude of the maximum strain. For brevity, these results have been omitted in this paper.

In Table 4 the column ‘Run label’ indicates the standard order of sixteen experimental run labels for different factor combinations as (1), *a, b, c, d, ab, ac, ad, bc, bd, cd, abc, abd, acd, bcd* and *abcd*. Numerical experiments are performed for each design combination and corresponding *FS* and percent strain are tabulated in Table 4. For runs 1, 2, 5 and 8, since *FS* is less than the unity, the failure occurs and consequently the node displacements are large. Percent strain value in these cases is unavailable because of the distorted grid.

Table 4

2.4. Regression models to obtain the performance functions

Based on the above results, regression models were developed for predicting *FS* as shown in Equations 8-10.

$$FS_{RMR50} = 0.0526 + 1.5083c + 0.0198\phi + 0.0298c\phi \quad (8)$$

$$FS_{RMR70} = -0.033 + 1.2636c + 0.024\phi + 0.0271c\phi \quad (9)$$

$$FS_{RMR90} = -0.2341 + 0.7118c + 0.0309\phi + 0.035c\phi \quad (10)$$

Equation 8 is for *RMR* = 50; Equation 9 is for *RMR* = 70 and Equation 10 is for *RMR* = 90. A comparison of *FS* between the predictions from Equations 8, 9 and 10 and the *FS* obtained from FLAC^{3D} is shown in Fig. 2. Considering that in SSR, the shear strength parameters *c* and ϕ are systematically reduced until failure, while *E* and K_0 have no influence on the global *FS*, a very accurate relationship was obtained between *FS* and *c* and ϕ with Coefficient of Determination R^2 equal to 1.0.

Fig. 2.

Similarly, the regression models for predicting the percent strain are shown in Equations 11-13.

$$\begin{aligned}\varepsilon_{RMR50}(\%) = {} & 0.2069 - 0.0827E_m - 0.0178\phi + 1.0526K_0 + 0.0536E_m c + \\ & 0.0028E_m\phi - 0.0253E_m K_0 - 0.005c\phi - 0.3529cK_0 - 0.0141\phi K_0\end{aligned} \quad (11)$$

$$\begin{aligned}\varepsilon_{RMR70}(\%) = {} & 0.0904 - 0.0058E_m - 0.4788c - 0.0044\phi + 0.292K_0 + 0.0046E_m c \\ & +0.0002E_m\phi - 0.002E_m K_0 + 0.0095c\phi - 0.0754cK_0 - 0.0035\phi K_0\end{aligned} \quad (12)$$

$$\begin{aligned}\varepsilon_{RMR90}(\%) = {} & 0.0113 - 0.0002E_m - 0.0699c - 0.0004\phi + 0.0478K_0 + \\ & 0.0002E_m c - 0.0001E_m K_0 + 0.0011c\phi - 0.0069cK_0 - 0.0004\phi K_0\end{aligned} \quad (13)$$

Equation 11 is for *RMR* = 50; Equation 12 is for *RMR* = 70 and Equation 13 is for *RMR* = 90. A comparison of the percent strain between the predictions from Equations 11, 12 and 13 and the values obtained from FLAC^{3D} is shown in Fig. 3. The above equations show the percent strain is a fairly nonlinear function of four parameters *c*, ϕ, E_m and K_0. For simplicity, only interactions between at most two of four variables are considered. Consequently because of the nonlinearity of the relationship between the parameters, R^2 slightly less than unity was obtained.

Fig. 3.

3. Probabilistic assessment of the limit states

In many civil engineering applications, the assessment of safety is made by first establishing a relationship between the load *S* of the system and the resistance *R*. The boundary separating the safe and 'failure' domains is the limit state surface (boundary) defined by $G(\mathbf{x}) = R - S = 0$, in which $\boldsymbol{x}$ = vector of the random variables. Mathematically, $R > S$ or $G(\boldsymbol{x}) > 0$ would denote a 'safe' domain. An unsatisfactory or 'failure' domain occurs when $R < S$ or $G(\boldsymbol{x}) < 0$. Calculation of P_f involves the determination of the joint probability distribution of *R* and *S* and the integration of the Probability Density Function (PDF) over the failure domain. Considering that the PDFs of the random variables are not known in most geotechnical applications and the integration is computationally demanding when multi-variables are involved, an approximate method, known as the First-Order Reliability Method (FORM) (Hasofer and Lind, 1974), is commonly used to assess P_f. The approach involves the transformation of the limit state surface into a space of standard normal uncorrelated variables, wherein the shortest distance from the transformed limit state surface to the origin of the reduced variables is the reliability index β (Cornell, 1969). For normal distributed random variables, $P_f \approx 1 - \Phi(\beta)$, in which Φ = cumulative normal density function. Table 1 shows the relationship between β and P_f. Mathematically, Low and Tang (2004) have shown that β can be computed using:

$$\beta = \min_{x \in \mathrm{F}} \sqrt{\left[\frac{x_i - \mu_i}{\sigma_i}\right]^T [\mathbf{R}]^{-1} \left[\frac{x_i - \mu_i}{\sigma_i}\right]} \tag{14}$$

in which x_i is the set of *n* random variables, μ_i is the set of mean values, σ_i is the standard deviation, **R** is the correlation matrix and *F* is the failure region. Low (1996) has shown that Microsoft EXCEL spreadsheet can be used to perform the minimization and determine β.

The reliability index β and the probability of failure P_f for both the ultimate and the serviceability limit states can be calculated using FORM spreadsheet method, as shown in Fig. 4 for *RMR* = 50. The EXCEL spreadsheet SOLVER function is used to search for the design point, also named the most probable failure point (Low and Tang,

2004). Detailed explanations of the setup of the spreadsheet for reliability calculations is described in section 3.3. The FORM spreadsheets for calculations of β and P_f for *RMR* = 70 and 90 can be compiled in the same way.

Fig. 4.

3.1. Probabilistic assessment of the ultimate limit states

The global *FS* is investigated first. Assuming the critical *FS* value is 1, the performance function for *RMR* = 50 is then given by

$$G(\mathbf{x})_{RMR50} = FS_{RMR50} - FS_{critical} = 0.0526 + 1.5083c + 0.0198\phi + 0.0298c\phi - 1 \quad (15)$$

The calculated β and P_f values for *RMR* = 70 and 90 can also be calculated in this way, and the only difference lies in the performance functions. The calculated β and P_f values for different *RMR* values are listed in Table 5. Table 5 indicates that the more is *RMR* (that means the rock mass is even more competent), the larger is the calculated β and the lower is the probability of an unstable underground cavern.

Table 5

3.2. Probabilistic assessment of the serviceability limit states

An appropriate value can be assigned to the percent strain threshold through the concept of critical strain. Sakurai (1986, 1997b) proposed a relationship between critical strain and Young's modulus *E* and Uniaxial Compressive Strength *UCS*, and suggested Fig. 5 and Fig. 6 as representing the limiting bounds for these relationships. These relationships are based on rock tests. However, Sakurai (1997b) showed that critical strain results for in-situ rock masses also fall within these bounding lines. Hazard warning levels for stability assessment of tunnels have been established by Sakurai on the basis of the relationship between critical strain and *UCS* in laboratory specimens and then subsequently confirmed through in-situ displacement monitoring. Hazard warning level II (Fig. 6) is coincident with the central line of the critical strain versus *UCS* limit zone, and represents the transition from a stable to unstable tunnel.

Fig. 5.

Fig. 6.

Table 6 shows the range of critical strain values obtained from the upper and lower bound curves in Fig. 5 and 6, and from the hazard warning level II in Fig. 6.

Table 6

The critical strains from the Hazard warning level II values are adopted except for *RMR* = 90. For *RMR* = 90, considering that the FLAC^{3D} calculated percent strain values are far below 0.19%, the critical strain value of 0.048%, obtained from the lower bound from Fig. 6 is employed. Thus the performance functions for the different *RMR* values are:

$$G(\mathbf{x})_{RMR50} = \varepsilon_{critical} - \varepsilon = 0.52 - (0.2069 - 0.0827E_m - 0.0178\phi + 1.0526K_0 + 0.0536E_m c + 0.0028E_m\phi - 0.0253E_m K_0 - 0.005c\phi - 0.3529cK_0 - 0.0141\phi K_0) \quad (16)$$

$$G(\mathbf{x})_{RMR70} = \varepsilon_{critical} - \varepsilon = 0.24 - (0.0904 - 0.0058E_m - 0.4788c - 0.0044\phi + 0.292K_0 + 0.0046E_m c + 0.0002E_m\phi - 0.002E_m K_0 + 0.0095c\phi - 0.0754cK_0 - 0.0035\phi K_0) \quad (17)$$

$$G(\mathbf{x})_{RMR90} = \varepsilon_{critical} - \varepsilon = 0.048 - (0.0113 - 0.0002E_m - 0.0699c - 0.0004\phi + 0.0478K_0 + 0.0002E_m c - 0.0001E_m K_0 + 0.0011c\phi - 0.0069cK_0 - 0.0004\phi K_0) \quad (18)$$

The calculated β and P_f values are listed in Table 7.

Table 7

Setting the critical strain values as the threshold percent strain, performance functions of the ultimate limit state can be obtained and used for reliability assessment. Comparison between Table 5 and Table 7 reveals that for the same *RMR*, serviceability limit states have a higher probability of occurrence than ultimate limit states. In addition, Table 8 lists the design points of the serviceability limit state. At these design points, the corresponding calculated *FS* values are given in Table 8. Table 8 indicates that at the design points of the serviceability limit state the calculated *FS* values are all greater than unity.

Table 8

3.3. System reliability

The reliability assessment is performed on the percent strain and the global *FS* criterion must be satisfied during the search for the design point. As shown in Fig. 7, Cells D5:G8 are parameters which are set corresponding to the variable distribution types. For normal distribution, Cells D5:D8 correspond to the mean values while Cells

E5:E8 correspond to the standard deviations. For nonnormal distributions, the nonnormal parameters are replaced by an equivalent normal ellipsoid, centered at the equivalent normal mean. The correlation matrix [***R***] Cells J5:M8 are used to define the correlations between *E*, *c*, ϕ and K_0. While the first three parameters are likely to be correlated as they are derived from the RMR system, for simplicity and illustrative purposes, the variables are assumed to be non-correlated. Analysis for correlated variables can be carried out through transforming the correlated variables to a set of uncorrelated variables for the correlation matrix R in Eq. (14) by finding the eigen-values and eigen-vectors. These procedures are detailed in Ang and Tang (1984). The n_i vector in Cells N5:N8 contains equations for $(x_i - \mu_i)/\sigma_i$ as defined in Eq. (14). Cell K11 contains the mathematical equation for serviceability limit state $G(\boldsymbol{x})_{RMR50} = \varepsilon_{critical} - \varepsilon_{RMR50}$. The regression models predicting *FS* (Equations 8, 9 or 10) are implemented into Cell B11 representing the constraint from global *FS*, in which mathematical expression of $FS - FS_{critical} \geq 0$ must be satisfied for each combination of parameters *c* and ϕ. The design point (x_i* values in Cells H5:H8) was obtained by using the EXCEL spreadsheet's built-in optimization routine SOLVER to minimize the cell, by changing the x_i* values, under the constraint that the performance function $G(x_i^*) = 0$. Prior to invoking the SOLVER search algorithm, the x_i* values were set equal to the mean values (10, 0.245, 29.5, 2.5) of the original four random variables. Iterative numerical derivatives and directional search for the design point x_i* are automatically carried out in the spreadsheet environment. Reliability indices β corresponding to different mean global *FS* can be calculated based on the FORM spreadsheet method described in Fig. 7 and are shown in Table 9. Fig. 8 illustrates the relationship between mean *FS* and β of serviceability limit under different *RMR*.

Fig. 7.

Table 9

Fig. 8.

Fig. 8 indicates that a target β = 3.0 (Target performance level: Above average) is achievable for a mean *FS* larger than 1.62 for *RMR* = 50. For *RMR* = 70, an above

average performance level is achievable for a mean *FS* larger than 1.86. The same performance level can also be achieved for *RMR* = 90 with a mean *FS* larger than 2.25. It is logical that the higher the quality of the rock mass, the larger the mean factor of safety. As Figs. 5 and 6 indicate, the higher the quality of the rock mass (higher Young's modulus and Uniaxial compressive strength), the smaller will be the percent strain to avert a given hazard level (Table 6). The constructed lines can be used as a preliminary design tool when selecting a required global *FS* provided the quality of rock mass and the in-situ stress are known.

It is obvious that optimal design in terms of avoiding over-design of rock mass is achievable if a certain level of risk is acceptable. Thus the procedures outlined in this paper can be used to obtain a rational optimal design of underground rock caverns. Based on Table 9 and Fig. 8, a global *FS* no less than the values proposed in Table 10 can be used to satisfy the target performance levels under different ground conditions. These *FS* values are also recommended to meet the performance level requirement under similar ground conditions. They can also be used as guidance with regard to the choice of a proper factor of safety for underground rock cavern.

Table 10

4. Conclusions

This paper illustrates an approach for underground rock cavern design utilizing quantitative probabilistic assessment with the use of the *RMR* system to determine the global *FS* required under different ground conditions and to quantify uncertainty in the analysis. The *RMR* classification system is used to derive the Mohr-Coulomb strength parameters through empirical correlations and equations. Finite Difference analysis using these strength parameters are performed to calculate the global *FS* and the percent strain, in accordance with the methodology of 2^k factorial design. Two polynomial regression models for the ultimate and serviceability limit states are developed for each ground condition.

For evaluating the serviceability limit state, the concept of critical strain is adopted to determine the threshold percent strain values under different ground conditions.

Through the use of the automated spreadsheet search algorithm to determine the design point, to meet the different target performance levels, the required minimum *FS* is obtained and termed as the critical value. The procedures outlined in this paper can be used to obtain a rational design of underground rock caverns. The *FS* values in Table 10 are also recommended for general project use under similar ground conditions.

This study will be extended to consider 3D underground caverns that account for rock reinforcements and excavation rate and sequence. In addition, geometrical situations of different caverns shapes and sizes will also be considered.

Acknowledgements

The authors would like to express their appreciation to the Defense Science and Technology Agency Singapore for providing the research funding for this research. The authors are most thankful to the two anonymous reviewers for their valuable comments and suggestions.

References

Aksoy, C.O., Ozacar, V. Kantarci,O., 2010. An example of estimating rock mass deformation around an underground opening using numerical modeling. Int. J. Rock. Mech. Min. Sci. 47(2), 272-278.

Ang, A.H.S., Tang, W.H., 1984. Probability concepts in engineering planning and design, Vol. II - Decision, risk and reliability, New York, John Wiley and Sons.

Barton, N., Løset, F., Lien, R., Lunde, J., 1980. Application of the Q-system in design decisions. In Subsurface space, New York: Pergamon. 2, 553-561.

Basarir, H., 2006. Engineering geological studies and tunnel support design at Sulakyurt dam site, Turkey. Engineering Geology 86(4), 225-237.

Basarir, H., 2008. Analysis of rock-support interaction using numerical and multiple regression modeling. Can. Geotech. J. 45, 1-13.

Bieniawski, Z. T., 1973. Engineering classification of jointed rock mass. Transactions of the South African Institution of Civil Engineers 15, 335-344.

Bieniawski, Z. T., 1974. Geo-mechanics classification of rock mass and its application to tunneling. Advance in rock mechanics 2A, 27-32.

Bieniawski, Z. T., 1978. Determining rock mass deformability: experience from case histories. Inter. J. Rock Mech. Min. Sci. Geomech. Abstr. 15, 237-247.

Bieniawski, Z. T., 1989. Engineering rock mass classifications. Wiley, Chichester.

Brinkgreve, R.B.J., Bakker, H.L., 1991. Non-linear finite element analysis of safety factors. Proc. 7th Int. Conf. on Computer Methods and Advances in Geomechanics, 1117-1122,

Cornell, C.A., 1969. A probability-based structural code. American Concrete Institute 66(12), 974-985.

Hammah, R.E., Yacoub, T., Curran, J.H., 2007. Serviceability-based slope factor of safety using the shear strength reduction (SSR) method. The Second Half Century of Rock Mechanics 11th Congress of the International Society for Rock Mechanics, Taylor & Francis, 1137-1140,

Hasofer, A.M., N. Lind, 1974. An exact & invariant first-order reliability format. Journal of Engineering Mechanics ASCE 100(1), 111-121.

Hoek, E., Brown, E.T., 1997. Practical estimates of rock mass strength. Int J Rock Mech Mining Sci Geomech 34(8), 1165-1186.

Low, B. K., 1996. Practical probabilistic approach using spreadsheet. In Uncertainty in the geologic environment, Ed. C.D. Shackelford, P.P. Nelson, & M.J.S. Roth, GSP 58, ASCE, Reston, 1284-1302.

Low, B. K., Tang, W. H., 2004. Reliability analysis using object-oriented constrained optimization. Structural Safety 26(1), 69-89.

Montgomery, D.C., 2001. Design and analysis of experiments, Singapore, Wiley.

Palmstrom, A., Broch, E., 2006. Use and misuse of rock mass classification systems with particular reference to the Q system. Tunn. Undergr. Space Technol. 21, 575-593.

Sakurai, S., 1986. Field measurement and hazard warning levels in NATM. Soils and foundation 34(2), 5-10.

Sakurai, S., 1997a. Lessons learned from field measurements in tunneling. Tunn. Undergr. Space Technol. 12(4), 453-460.

Sakurai, S., 1997b. Strength parameters of rocks determined from back analysis of measured displacements. In: First Asian Rock Mechanics Symposium, ISRM. Seoul, 95-99.

Sakurai, S., Akutagawa, S., Takeuchi, K, Shinji, M., Shimizu, N., 2003. Back analysis for tunnel engineering as a modern observational method. Tunnelling and Underground Space Technology 18, 185-196.

Serafim, J.L., Pereira, J.P., 1983. Considerations on the geomechanical classification of Bieniawski. Int. Symp. Engineering Geology and Underground Construction. Lisbon, A.A. Balkema, Rotterdam. 1, II.33- II.42.

Sharifzadeh, M., Daraei, R., Broojerdi, M.S., 2011. Design of sequential excavation tunneling in weak rocks through findings obtained from displacements based back analysis. Tunnelling and Underground Space Technology 28, 10-17.

Trueman, R., 1988. An evaluation of strata support techniques in dual life gateroads. University of Wales (Ph.D. thesis), Cardiff, UK.

U.S. Army Corps of Engineers., 1997. Engineering and design: introduction to probability and reliability methods for use in geotechnical engineering. Department of the Army, Washington, D.C. Engineer Technical Letter, 1110-2-547.

Vermeer, P.A., Ruse, N., Marcher, T., 2002. Tunneling heading stability in drained ground. Felsbau, Jg. 20(6), 8-18.

Vermeer, P.A., Ruse, N., 2002. Neue Entwicklungen in der Tunnelstatik. Proc. 3rd Kolloquium Bauen in Boden und Fels, Technische Akademie Esslingen 3-14. Ostfildern: TAE.

Zienkiewicz, O.C., Humpheson, C., Lewis, R.W., 1975. Associated and non-associated visco-plasticity in soil mechanics. Geotechnique 25(4), 671-689.

Table captions

Table 1 Target reliability indices (U.S. Army Corps of Engineers, 1997)

Table 2 *RMR* values, rock class, empirical estimates and assumed values of rock strength parameters

Table 3 Input parameters for the 2^4 factorial design

Table 4 Observations from numerical experimentations for 2^4 factorial design

Table 5 β and P_f values of ultimate limit state for different *RMR* values

Table 6 Critical strains derived from Sakurai's relationships (Fig. 5 and Fig. 6)

Table 7 β and P_f values of serviceability limit state for different *RMR* values

Table 8 Calculated *FS* values at the design points of serviceability limit state

Table 9 Calculation results of β corresponding to mean *FS* under different *RMR*

Table 10 Recommended *FS* values for target performance levels under different *RMR* values

Table 1 Target reliability indices (U.S. Army Corps of Engineers, 1997)

Reliability index β	Probability of failure $P_f \approx 1 - \Phi(\beta)$	Expected performance level
1.0	0.16	Hazardous
1.5	0.07	Unsatisfactory
2.0	0.023	Poor
2.5	0.006	Below average
3.0	0.001	Above average
4.0	0.00003	Good
5.0	0.0000003	High

Table 2 *RMR* values, rock class, empirical estimates and assumed values of rock strength parameters

Average *RMR*	Rock Class (*RMR* range)	Stochastic Variables			Deterministic parameters			
		E_m (GPa)	c (kPa)	ϕ (°)	ρ (kg/m^3)	ν	σ_{cm} (MPa)	σ_t (MPa)
50	Fair (41-60)	10.00	0.245	29.5	2430	0.24	10.04	1.00
70	Good (61-80)	31.62	0.345	39.5	2610	0.24	33.34	3.33
90	Very Good (81-100)	100.00	0.445	49.5	2650	0.24	110.70	11.07

Table 3 Input parameters for the 2^4 factorial design

Random variables	Distribution type	Notation	*RMR*	Mean	*COV*	*S.D.*	High level	Low level
E_m (GPa)	Normal	A	50	10.00	0.2	2.00	13.29	6.71
			70	31.62	0.2	6.32	42.03	21.22
			90	100.00	0.2	20.00	132.90	67.10
c (MPa)	Normal	B	50	0.245	0.2	0.049	0.326	0.164
			70	0.345	0.2	0.069	0.459	0.231
			90	0.445	0.2	0.089	0.591	0.299
ϕ (°)	Normal	C	50	29.5	0.15	4.43	36.78	22.22
			70	39.5	0.15	5.93	49.25	29.75
			90	49.5	0.15	7.43	61.71	37.29
K_0	Normal	D	—	2.5	0.12	0.30	3.0	2.0

Table 4 Observations from numerical experimentations for 2^4 factorial design

Run No.	A	B	C	D	Run label	*RMR* = 50		*RMR* = 70		*RMR* = 90	
						FS	Percent Strain (%)	*FS*	Percent Strain (%)	*FS*	Percent strain (%)
1	-	-	-	-	(1)	0.85	—	1.16	0.1572	1.52	0.0288
2	+	-	-	-	a	0.85	—	1.16	0.0799	1.52	0.0145
3	-	+	-	-	b	1.20	0.6409	1.63	0.1073	2.11	0.0199
4	-	-	+	-	c	1.21	0.3331	1.75	0.0568	2.53	0.0149
5	-	-	-	+	d	0.85	—	1.16	0.3096	1.52	0.0537
6	+	+	-	-	ab	1.20	0.3232	1.63	0.0545	2.11	0.0100
7	+	-	+	-	ac	1.21	0.1666	1.75	0.0289	2.53	0.0075
8	+	-	-	+	ad	0.85	—	1.16	0.1564	1.52	0.0272
9	-	+	+	-	bc	1.63	0.2500	2.34	0.0424	3.37	0.0143
10	-	+	-	+	bd	1.20	1.1282	1.63	0.2156	2.11	0.0397
11	-	-	+	+	cd	1.21	0.6275	1.75	0.0977	2.53	0.0231
12	+	+	+	-	abc	1.63	0.1255	2.34	0.0215	3.37	0.0072
13	+	+	-	+	abd	1.20	0.5666	1.63	0.1099	2.11	0.0200
14	+	-	+	+	acd	1.21	0.3158	1.75	0.0497	2.52	0.0116
15	-	+	+	+	bcd	1.63	0.4725	2.34	0.0812	3.37	0.0223
16	+	+	+	+	abcd	1.63	0.2369	2.34	0.0412	3.37	0.0112

Table 5 β and P_f values of ultimate limit state for different *RMR* values

RMR	β	P_f (%)
50	1.358	8.729
70	3.016	0.128
90	3.719	0.010

Table 6 Critical strains derived from Sakurai's relationships (Fig.5 and Fig. 6)

RMR	Statistics	E_m (GPa)	σ_{cm} (MPa)	Critical strain (%)		
				From Fig. 5	From Fig. 6	Hazard warning level II (from Fig. 6)
50	Mean	10.00	10.04	0.11-0.9	0.16-1.6	0.52
	Minimum	6.71	—	0.15-1.0	—	
	Maximum	13.29	—	0.10-0.8	—	
70	Mean	31.62	33.34	0.08-0.7	0.09-0.9	0.24
	Minimum	21.22	—	0.09-0.75	—	
	Maximum	42.03	—	0.07-0.6	—	
90	Mean	100.00	110.70	0.06-0.5	0.048-0.48	0.19
	Minimum	67.10	—	0.065-0.55	—	
	Maximum	132.90	—	0.05-0.4	—	

Table 7 β and P_f values of serviceability limit state for different *RMR* values

RMR	β	P_f (%)
50	0.006	49.768
70	1.504	6.626
90	1.564	5.890

Table 8 Calculated *FS* values at the design points of serviceability limit state

RMR	Design points of serviceability limit state	*FS* values at the design point
50	(9.993, 0.245, 29.48, 2.501)	1.221
70	(27.88, 0.311, 33.72, 2.755)	1.454
90	(65.59, 0.384, 36.37, 2.946)	1.652

Table 9 Calculation results of β corresponding to mean *FS* under different *RMR*

Rock Mass Conditions	Critical Strain (%)	*FS* and corresponding Serviceability Reliability Index β									
Fair	0.52	*FS*	1.35	1.36	1.43	1.49	1.50	1.55	1.56	1.61	1.62	1.75
RMR = 50		β	0.94	1.02	1.54	2.00	2.07	2.46	2.54	2.93	3.01	4.05
Good	0.24	*FS*	1.45	1.66	1.67	1.76	1.77	1.85	1.86	1.94	2.01	2.02
RMR = 70		β	1.50	1.99	2.03	2.47	2.52	2.97	3.03	3.51	3.96	4.02
Very Good	0.048	*FS*	1.77	1.96	2.00	2.24	2.25	2.26	2.51	2.52	2.74	2.75
RMR = 90		β	2.53	2.62	2.66	2.98	3.00	3.02	3.49	3.51	3.99	4.02

Table 10 Recommended *FS* values for target performance levels under different *RMR* values

Ground conditions	Target Performance Level and corresponding required *FS*			
	Poor	Below Average	Above Average	Good
Fair (*RMR* = 50)	1.49	1.56	1.62	1.75
Good (*RMR* = 70)	1.67	1.77	1.86	2.02
Very Good (*RMR* = 90)	1.77	1.77	2.25	2.75

Figure captions

Fig. 1. Cavern configuration, boundary fixity and detailed cavern periphery

Fig. 2. Comparisons between the target *FS* and the predicted *FS* for different *RMR*

Fig. 3. Comparisons between the target percent strain and the predicted value for different *RMR*

Fig. 4. Calculation on β and P_f of ultimate and serviceability limit states using FORM spreadsheet (for *RMR* = 50)

Fig.5. Sakurai's relationship between critical strain and Young's modulus (adapted from Sakurai, 1997b)

Fig.6. Sakurai's relationship between critical strain and *UCS*, also showing hazard warning level II for assessing the stability of tunnels (adapted from Sakurai 1986, 1997b)

Fig.7. Calculation on the system reliability using FORM spreadsheet for *RMR* = 50

Fig.8. Relationship between β and mean *FS* under different *RMR*

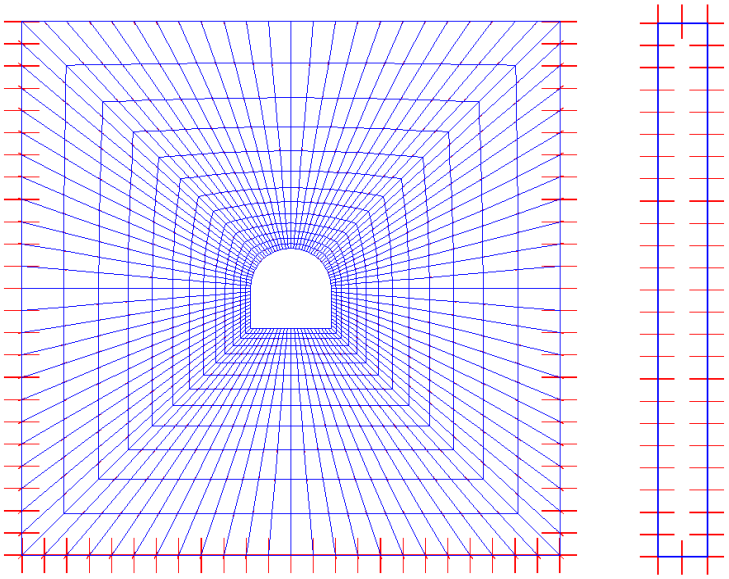

(a) Cavern configuration, boundary fixity and side view

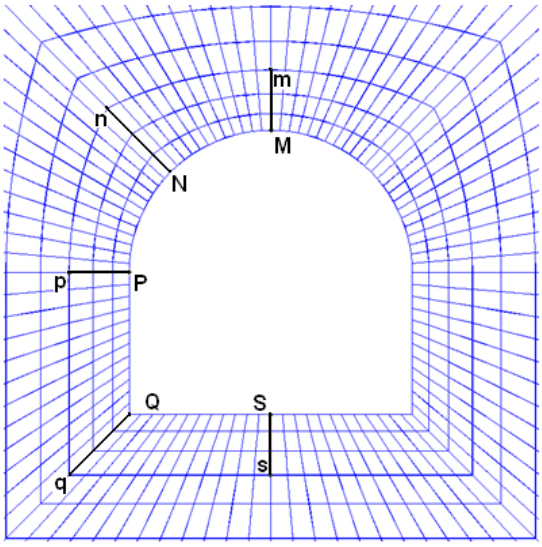

(b) Detailed cavern periphery

Fig.1. Cavern configuration, boundary fixity and detailed cavern periphery

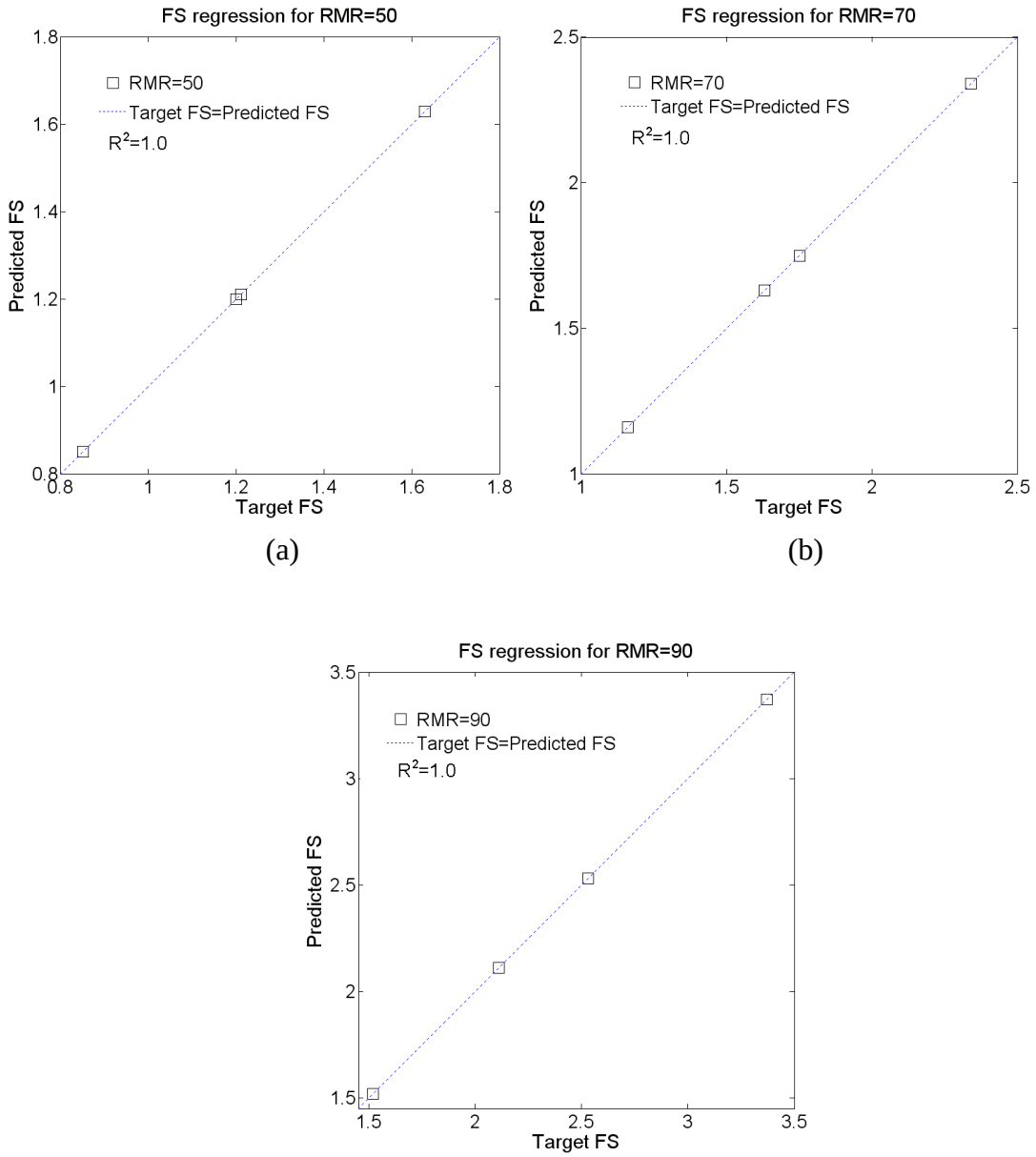

Fig. 2. Comparisons between the target *FS* and the predicted *FS* for different *RMR*

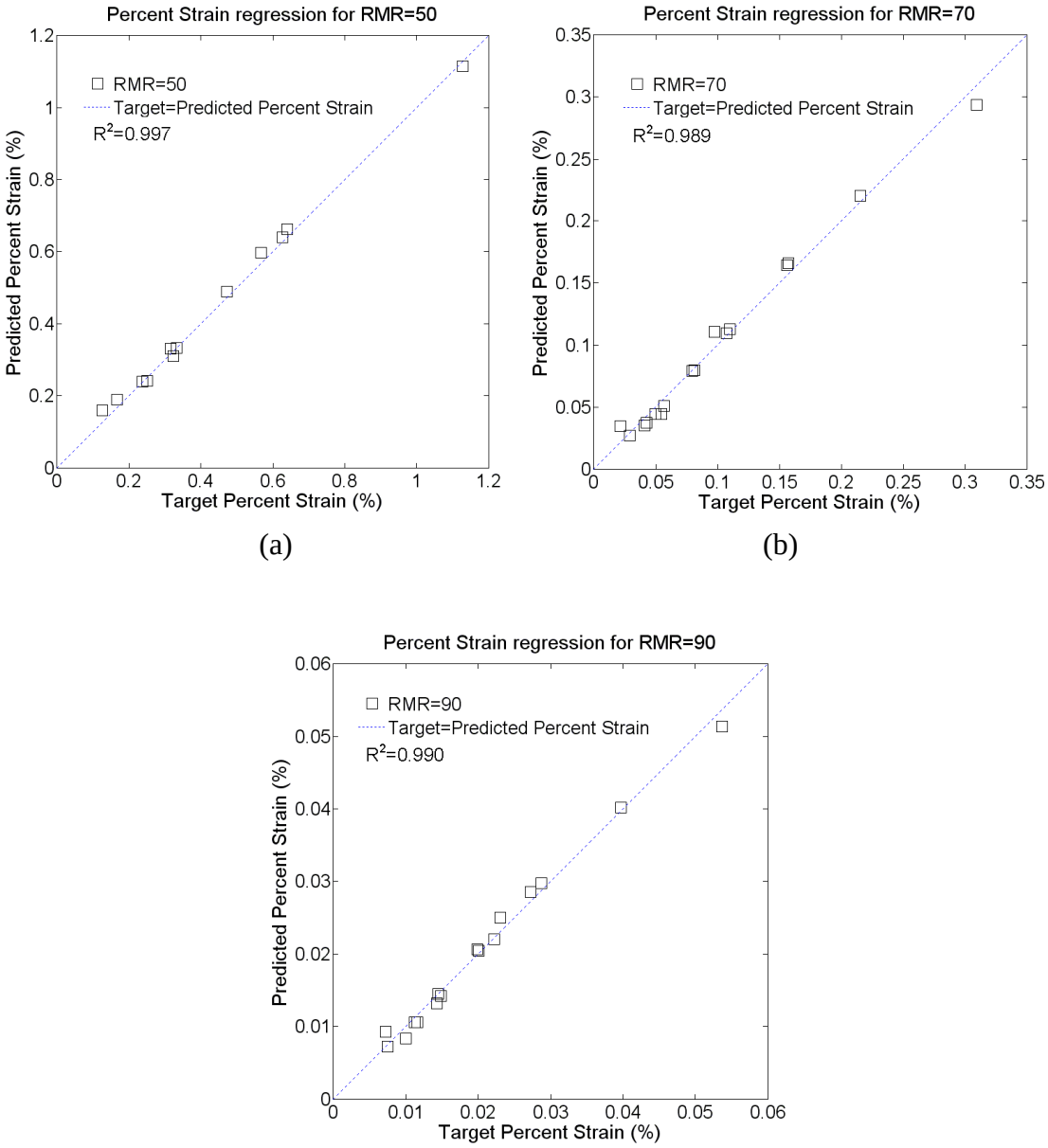

Fig.3. Comparisons between the target percent strain and the predicted value for different *RMR*

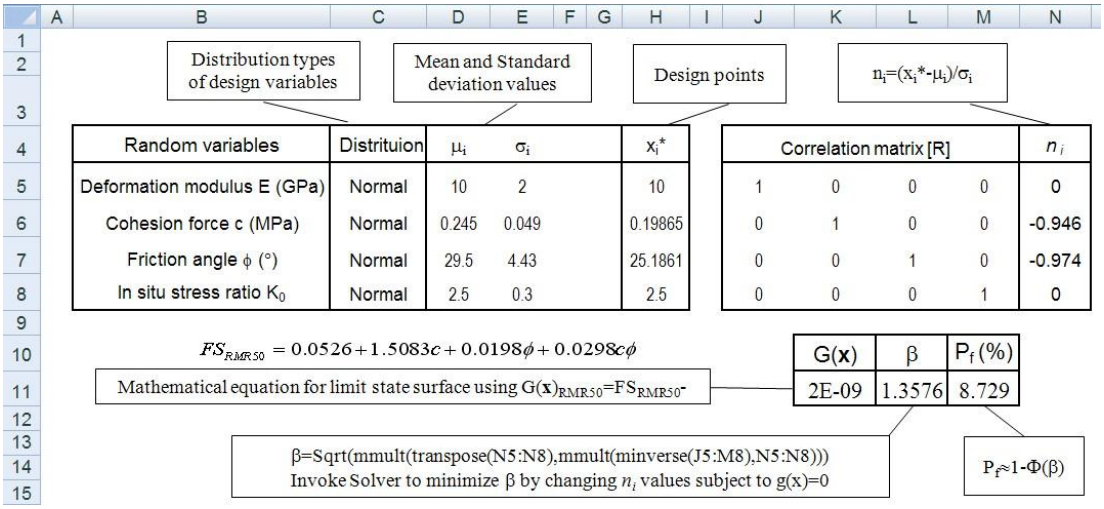

(a) Calculation on β and P_f for ultimate limit state

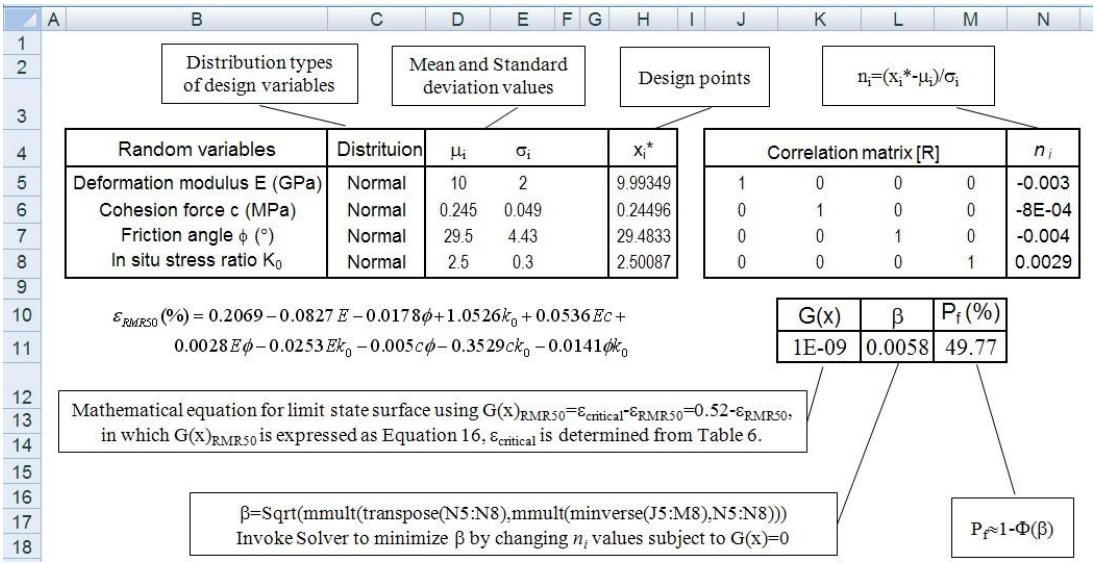

(b) Calculation on β and P_f for serviceability limit state

Fig.4. Calculation on β and P_f of ultimate and serviceability limit states using FORM spreadsheet (for *RMR* = 50)

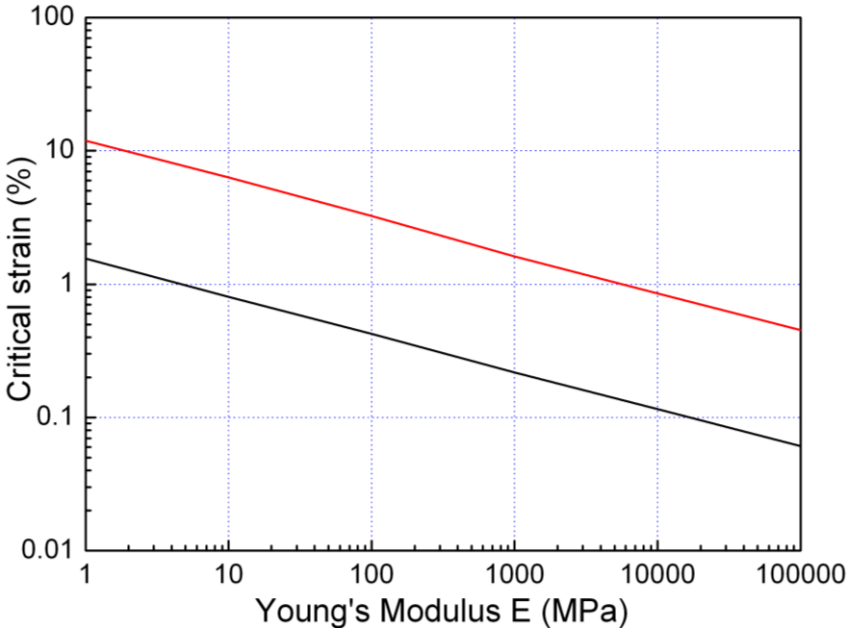

Fig.5. Sakurai's relationship between critical strain and Young's modulus E_m (adapted from Sakurai, 1997b)

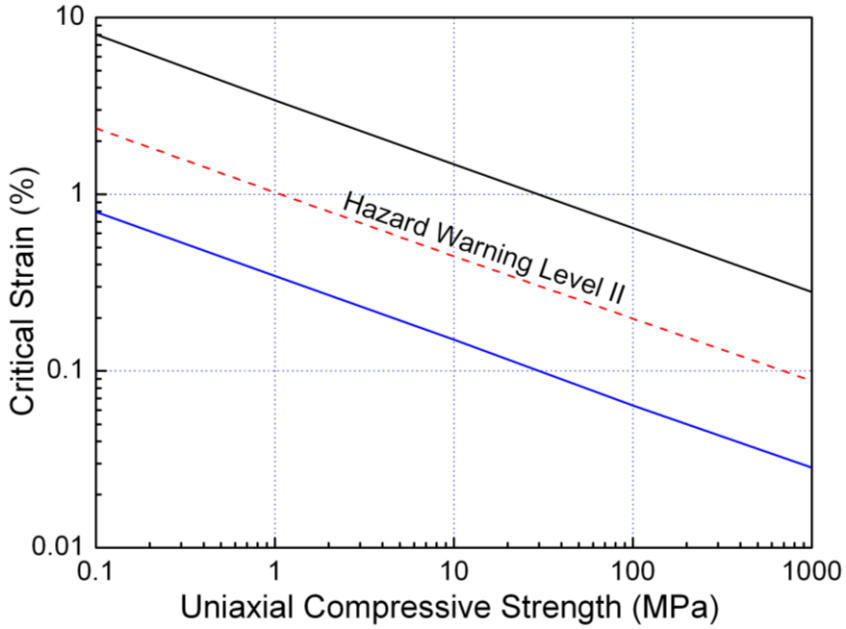

Fig.6. Sakurai's relationship between critical strain and *UCS*, also showing hazard warning level II for assessing the stability of tunnels (adapted from Sakurai 1986, 1997b)

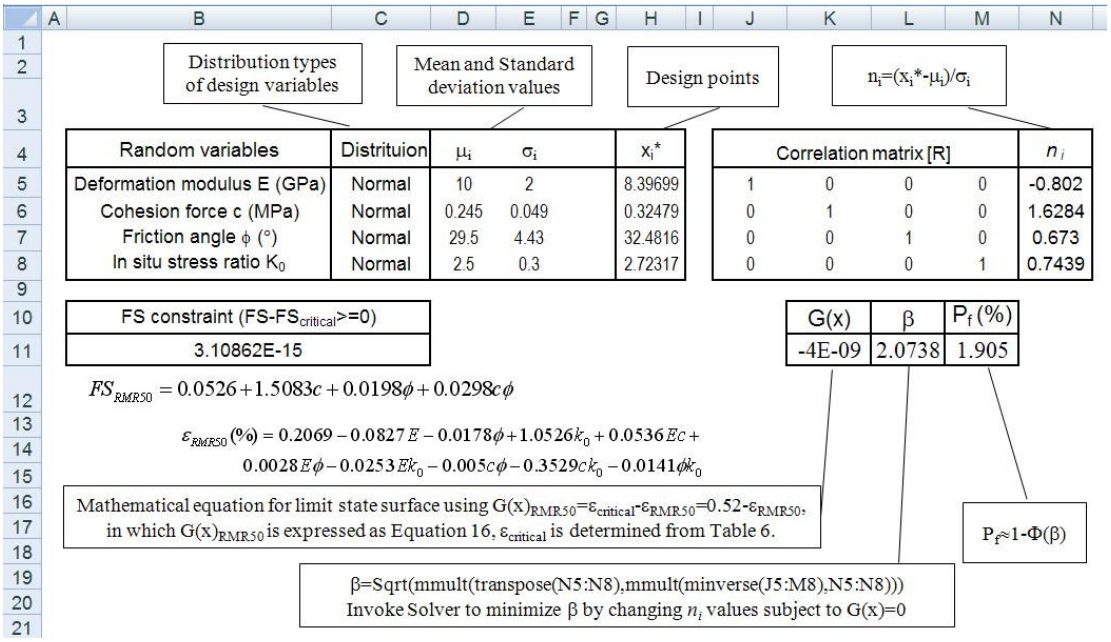

Fig.7. Calculation on the system reliability using FORM spreadsheet for *RMR* = 50

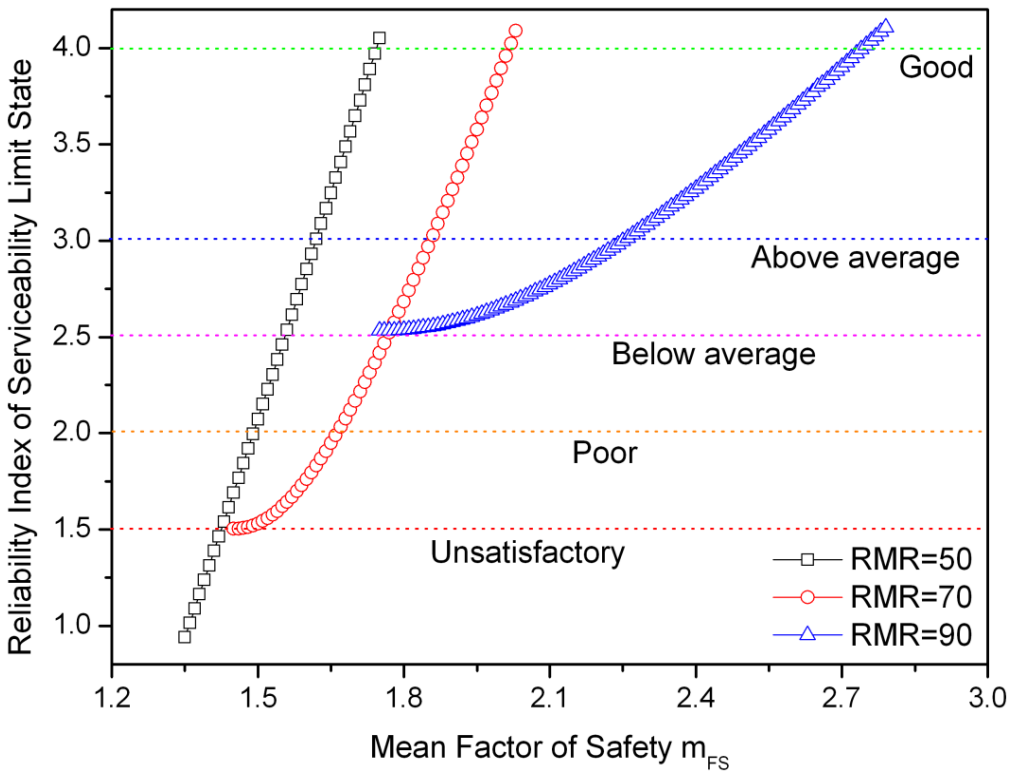

Fig.8. Relationship between β and mean *FS* under different *RMR*